

Example Problem CO2E-2

Estimation of the CO₂ Storage Capacity of a Brine Aquifer (Modified Stuttgart #3)

Abstract: *Estimation of the CO₂ storage capacity is investigated for CO₂ injection into a single-layer formation. The processes modeled include advective, multiphase flow, dissolution of CO₂ into the ambient brine, and non-isothermal effects due to temperature gradients within the formation. This problem is based on Problem 3 of the benchmark study first presented at the Workshop on Numerical Models for CO₂ Storage in Geological Formations in Stuttgart, Germany, and focuses on an injection scenario where CO₂ injection is located near a fault zone (Class, et al., 2009).*

Problem Description

This short course problem was developed based on Class et al. (2007) and Class et al. (2009). The problem describes the importance of being able to estimate a reservoir's storage capacity via the injection and subsequent migration in the formation, even after the injection period has been terminated. In addition to modeling the multiphase flow system, CO₂ dissolution in formation brine and temperature impacts are also considered. The conceptual model in the benchmark study is based on the Johansen formation off the coast of Norway. The injection well, which is represented as a source term in this short course problem, is located near a fault zone as shown in Figure 1. The original conceptual model includes nine separate layers, which has been modified here as a single layer problem to reduce the execution time for the simulations. This also reduces the complexity of the conceptual model, and increases the footprint of the CO₂ plume. The domain's lateral dimensions are approximately 9,600 x 8,900 m, with a variable thickness in Z. Porosity and permeability are represented as heterogeneous distributions.

CO₂ is injected into the bottom of the formation at a well located at x=5440 m (i=48) and y=3300 m (j=30). CO₂ is injected at a rate of 3.0 kg/s and a temperature of 80 °C over a period of 25 years, after which time the source is

turned off. The simulation of the evolution of the CO₂ plume continues for an additional 25 years, bringing the total simulation time to 50 years.

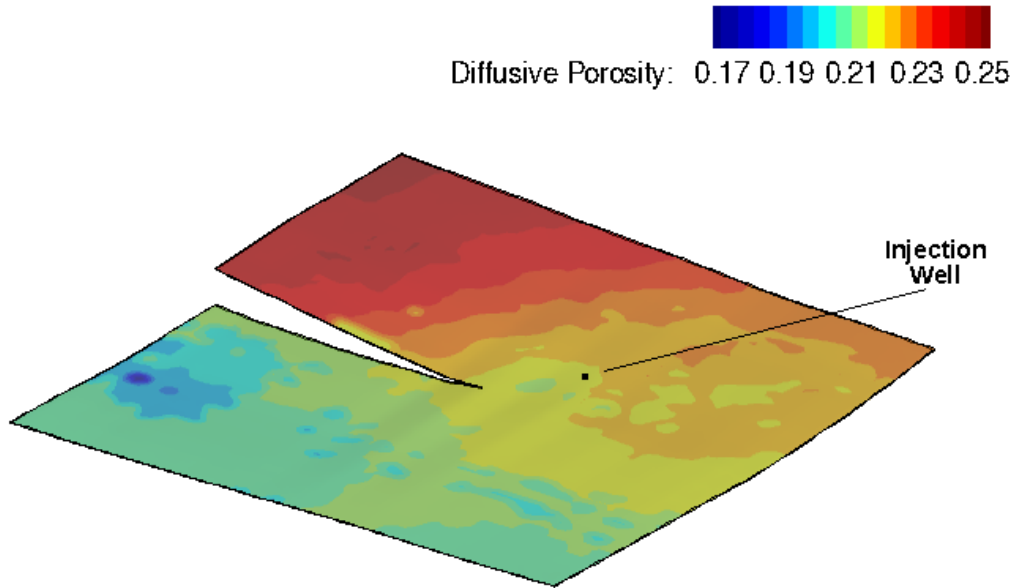


Figure 1. Location of Injection Well Within the Model Domain

The initial conditions in the domain are established using a hydrostatic pressure distribution that is dependent on the brine density and a geothermal temperature distribution. The initial temperature at 3000 m depth is 100 °C, and the geothermal gradient is 0.03 °C/m. The entire formation has an initial brine salinity of 0.1 kg/kg.

The top and bottom boundaries of the domain are set for no-flow conditions for aqueous and gas flow and salt transport. The lateral boundary conditions are constant Dirichlet conditions and equal to the initial conditions. This also holds for the faces of the fault which is intended to represent an infinitely permeable fault.

The primary output of interest is the mass of CO₂ in the formation over time. The total mass within the domain is tracked via the reference quantity specification (*Integrated CO2 Mass, Aqueous and Gas*) in the *Output Options Card*.

After 50 years of simulation, some amount of CO₂ may migrate over the open boundaries, depending on the permeability distribution within the domain. Plot file requests are made to enable the plotting of the plume development over time (Figure 2). Additional state variables, such as pressure and temperature can also be plotted as spatial distributions over time.

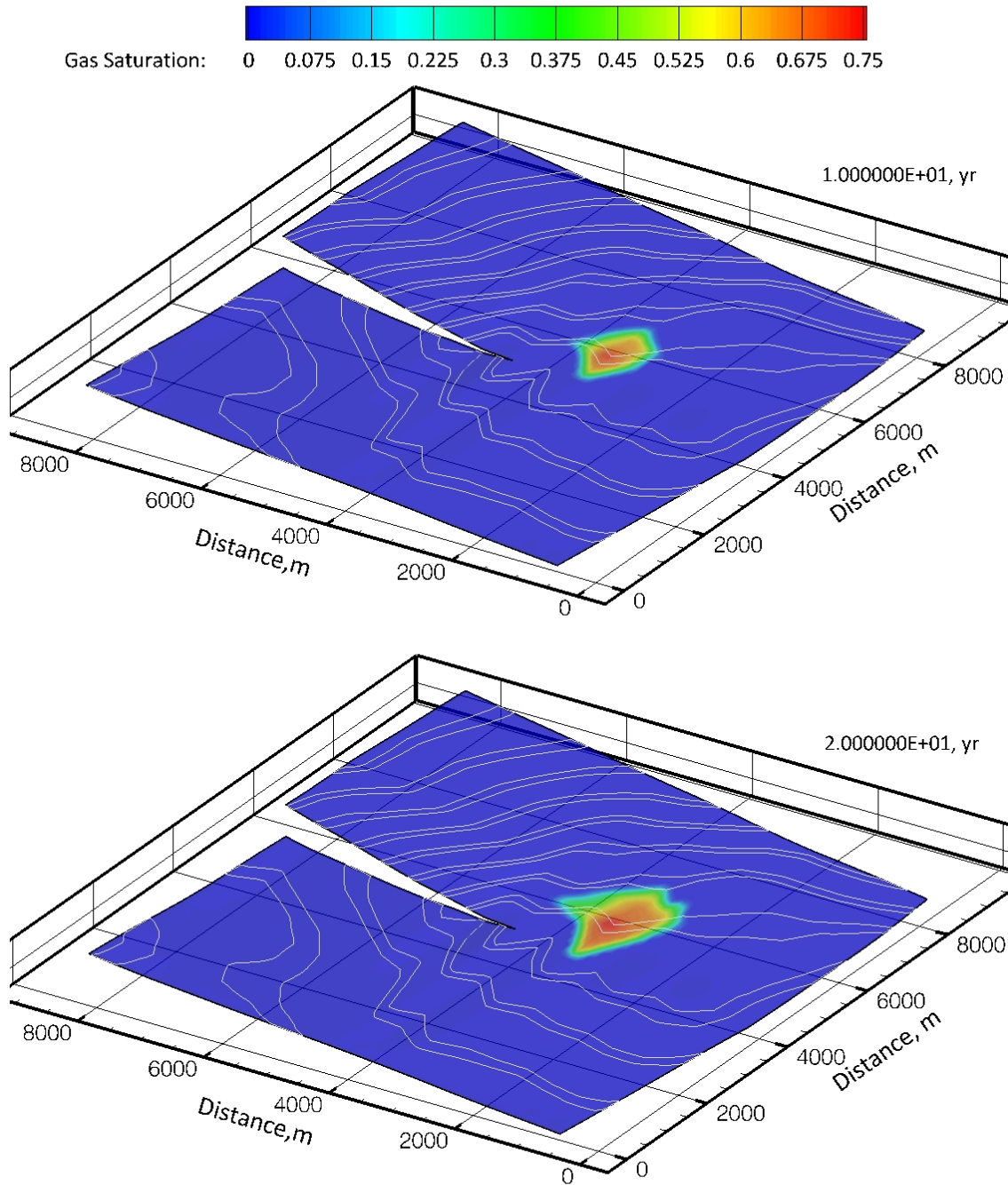


Figure 2a. CO₂ Gas Saturation at 10 and 20 years.

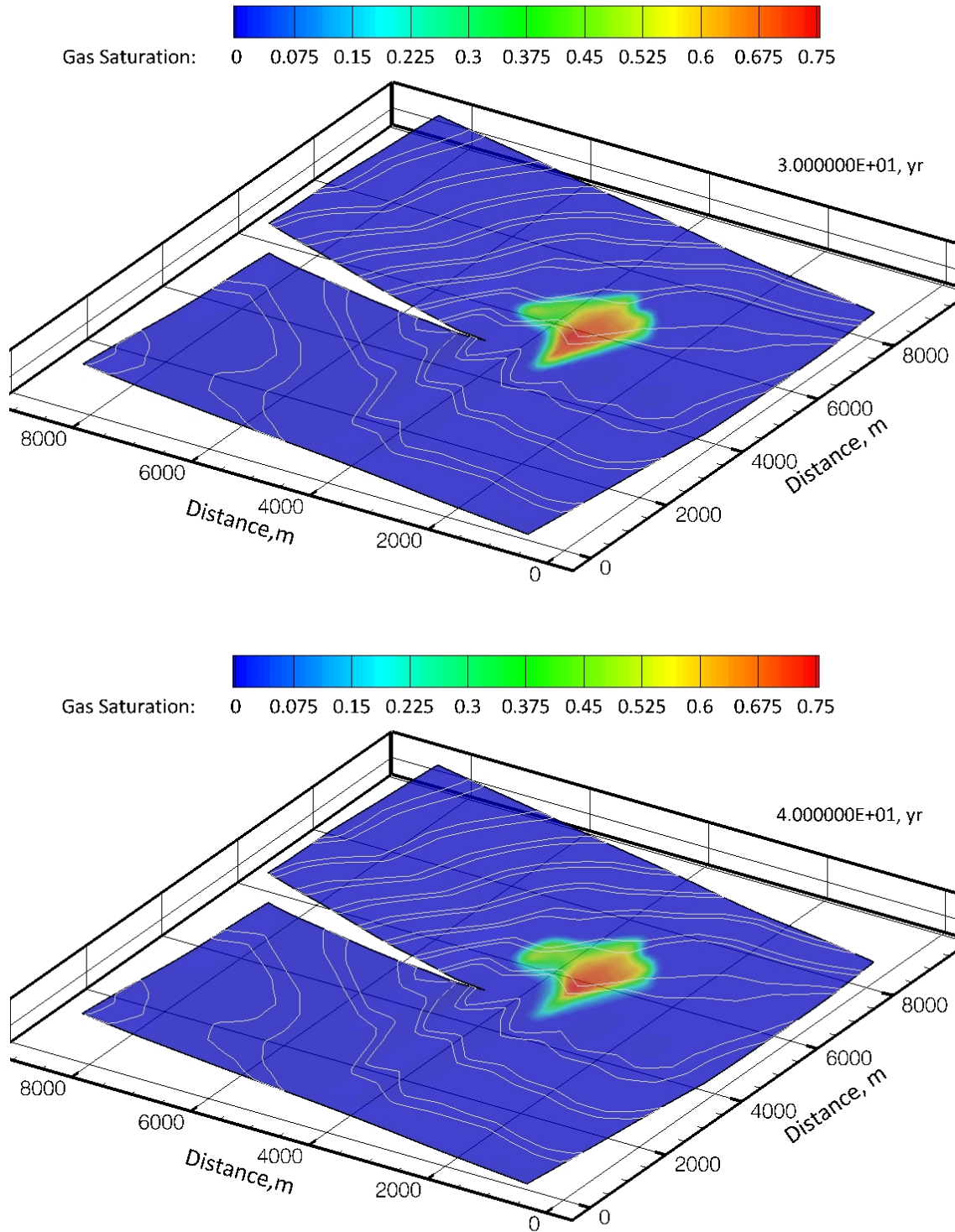


Figure 2b. CO₂ Gas Saturation at 30 and 40 years.

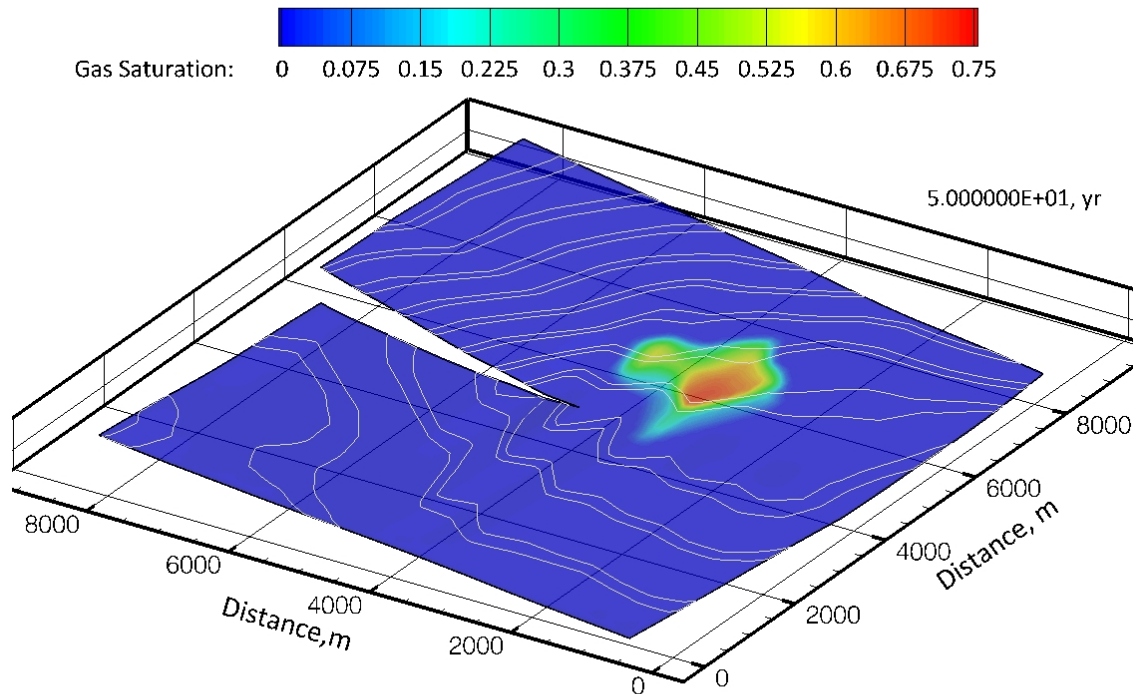


Figure 2c. CO₂ Gas Saturation at 50 years.

References

Class, H., A. Ebigbo, R. Helmig, H. K. Dahle, J. M. Nordbotten, M. A. Celia, P. Audigane, M. Darcis, J. Ennis-King, Y. Fan, B. Flemisch, S. E. Gasda, M. Jin · S. Krug, D. Labregere, A. N. Beni, R. J. Pawar, A. Sbai, S. G. Thomas, L. Trenty, L. Wei. 2009. "A benchmark study on problems related to CO₂ storage in geologic formations," *Comput. Geosci.*, 13:409-434.

Class, H., H. Dahle, F. Riis, A. Ebigbo and G. Eigestad. 2007. *Numerical Investigations of CO₂ Sequestration in Geological Formations: Problem-Oriented Benchmarks*. Universitat Stuttgart.

Exercises

1. (Basic) Execute the base case simulation with the porosity and permeability distributions defined in the input file. Generate a series of gas saturation profiles showing the evolution of the CO₂ plume over time. Identify the total amount of CO₂ injected into the aquifer, and the amount of CO₂ that exits the boundary.
2. (Moderate) Execute the base case simulation but decrease the injection

rate to identify the difference in the plume evolution and the amount of CO₂ that exits the open boundary of the domain. Examine the CO₂ plume extent and the amount of CO₂ stored in the aquifer.

3. (Moderate) Execute the base case simulation with different porosity and permeability distributions. This can be accomplished by changing the file specification for porosity and/or permeability. The base case simulation specifies porosity_9.dat and perm_9.dat. Porosity and permeability distributions corresponding to the other 8 layers that were part of the original benchmarking problem can be used to identify the impact to CO₂ plume migration and the impact on the amount of CO₂ stored within the domain.
4. (Moderate) Execute the base case simulation, but account for trapped gas saturation, assuming a maximum actual trapped gas saturation of 0.2. Plot the distribution of CO₂ mass over time in the domain as total, aqueous, gas, and trapped gas. Generate plots showing the extent and evolution of trapped and free gas over time.

Input Files

Basecase Simulation Input File

~Simulation Title Card
1,
STOMP Example Problem CO2E-2,
M.D. White,
Pacific Northwest Laboratory,
02 December 2011,
15:07 PST,
2,
Estimation of the CO2 Storage Capacity of
a Geological Formation.

~Solution Control Card
Normal,
STOMP-CO2e,
1,
0,s,50,yr,100.0,s,1.0,yr,1.25,16,1.e-06,
10000,
Variable Aqueous Diffusion,
Variable Gas Diffusion,
0,

~Grid Card
Element and Vertices,
78,78,1,

vertices_johansen_stomp.dat,49928,
elements_johansen_stomp.dat,

~Rock/Soil Zonation Card
IJK Indexing,

~Mechanical Properties Card
IJK Indexing,2650,kg/m³,file:porosity_9.dat,file:porosity_9.dat,Compressibility,1.e-9,1/psi,,,constant,1.0,1.0,

~Hydraulic Properties Card
IJK Indexing,file:perm_9.dat,mD,file:perm_9.dat,mD,file:perm_9.dat,mD,

~Saturation Function Card
IJK Indexing,Brooks and Corey,1.021,m,2.0,0.2,,

~Aqueous Relative Permeability Card
IJK Indexing,Free Corey,1.0,4.0,0.2,0.5,

~Gas Relative Permeability Card
IJK Indexing,Corey,0.2,0.05,1.0,

~Thermal Properties Card
IJK Indexing,parallel,3.5,W/m K,3.5,W/m K,3.5,W/m K,750,J/kg K,

~Salt Transport Card
IJK Indexing,0.0,m,0.0,m,

~Initial Conditions Card
Hydrostatic,32.0,MPa,-3169.5,m,100.0,C,-3000.0,m,-0.03,C/m,0.1,-3000.0,m,0.0,1/m,

~Source Card
1,
Gas Mass Source,Water-Vapor Mass Fraction,48,48,30,30,1,1,2,
0.0,yr,80.0,C,30.0,MPa,3.0,kg/s,0.0,
25.0,yr,80.0,C,30.0,MPa,3.0,kg/s,0.0,

~Boundary Conditions Card
8,
West,Energy Geothermal Gradient,Aqu. Initial Condition,Gas Initial Condition,Aqu. Mass Frac.,
1,1,1,78,1,1,1,
0,s,100.0,C,-3000.0,m,-0.03,C/m,,,,,0.1,,
East,Energy Geothermal Gradient,Aqu. Initial Condition,Gas Initial Condition,Aqu. Mass Frac.,
78,78,1,78,1,1,1,
0,s,100.0,C,-3000.0,m,-0.03,C/m,,,,,0.1,,
South,Energy Geothermal Gradient,Aqu. Initial Condition,Gas Initial Condition,Aqu. Mass Frac.,
1,78,1,1,1,1,
0,s,100.0,C,-3000.0,m,-0.03,C/m,,,,,0.1,,
North,Energy Geothermal Gradient,Aqu. Initial Condition,Gas Initial Condition,Aqu. Mass Frac.,
1,78,78,78,1,1,1,
0,s,100.0,C,-3000.0,m,-0.03,C/m,,,,,0.1,,
West,Energy Geothermal Gradient,Aqu. Initial Condition,Gas Initial Condition,Aqu. Mass Frac.,
40,40,40,78,1,1,1,
0,s,100.0,C,-3000.0,m,-0.03,C/m,,,,,0.1,,
East,Energy Geothermal Gradient,Aqu. Initial Condition,Gas Initial Condition,Aqu. Mass Frac.,
39,39,40,78,1,1,1,
0,s,100.0,C,-3000.0,m,-0.03,C/m,,,,,0.1,,
Bottom,Energy Geothermal Gradient,Aqu. Zero Flux,Gas Zero Flux,Salt Zero Flux.,

1,78,1,78,1,1,1,
0,s,100.0,C,-3000.0,m,-0.03,C / m,,,,,,,,,
Top,Energy Geothermal Gradient,Aqu. Zero Flux,Gas Zero Flux,Salt Zero Flux.,
1,78,1,78,1,1,1,
0,s,100.0,C,-3000.0,m,-0.03,C / m,,,,,,,,,

~Output Options Card

1,
48,30,1,
1,1,yr,m,6,6,6,
16,
Temperature,C,
Gas Saturation,,
Integrated CO2 Mass,MMT,
Integrated CO2 Aqueous,MMT,
Integrated CO2 Gas,MMT,
Aqueous Relative Permeability,,
Gas Relative Permeability,,
Salt Aqueous Mass Fraction,,
Salt Saturation,,
CO2 Aqueous Mass Fraction,,
CO2 Gas Mass Fraction,,
Gas Pressure,MPa,
Gas Density,,
Aqueous Density,kg / m^3,
Aqueous Pressure,MPa,
Diffusive Porosity,,
13,
1,yr,
2,yr,
3,yr,
4,yr,
5,yr,
10,yr,
15,yr,
20,yr,
25,yr,
30,yr,
35,yr,
40,yr,
45,yr,
14,
Temperature,C,
Gas Saturation,,
X Intrinsic Permeability,mD,
XNC Aqueous Volumetric Flux,m / s,
YNC Aqueous Volumetric Flux,m / s,
ZNC Aqueous Volumetric Flux,m / s,
Aqueous Relative Permeability,,
Gas Relative Permeability,,
Salt Aqueous Mass Fraction,,
Gas Pressure,MPa,
Gas Density,,
Aqueous Density,kg / m^3,
Aqueous Pressure,MPa,
Diffusive Porosity,,

Solutions to Selected Exercises

Exercise 1

Using the porosity and permeability distributions for layer 9, the total integrated mass of CO₂ in the system when CO₂ injection ceases is 2.37 MMT, as observed in the output file, under the integrated CO₂ mass column. Between 25 and 50 years, this mass remains constant, indicating that no CO₂ is transported across the open boundary on the eastern side of the domain. Time-series plots of the spatial distribution of the gas saturation show how the plume evolves over time, as shown in Figures 2a, 2b, and 2c. The distribution of mass, however, evolves over time with the aqueous CO₂ mass increasing and the gas CO₂ mass decreasing with time, as observed in the output file, under the integrated aqueous and gas CO₂ mass columns, or as shown in Figure 3.

Exercise 2

For these simulations the CO₂ is injected into a single node at a constant rate via the Source Card. To reduce the injection rate from 3.0 to 1.0 kg/s, the Source Card is altered for both time entries, where the first time entry is the start time for the source and the second time entry is the stop time for the source. The injection rate is interpolated between the two times, but with both rates being the same, the source is injected at a constant rate. With a lower injection rate the plume shape is more strongly impacted by gravitational forces during the injection period, compared with the base case, as shown in the time-series plots of the spatial distribution of the gas saturation show how the plume evolves over time, Figures 4a, 4b, and 4c.

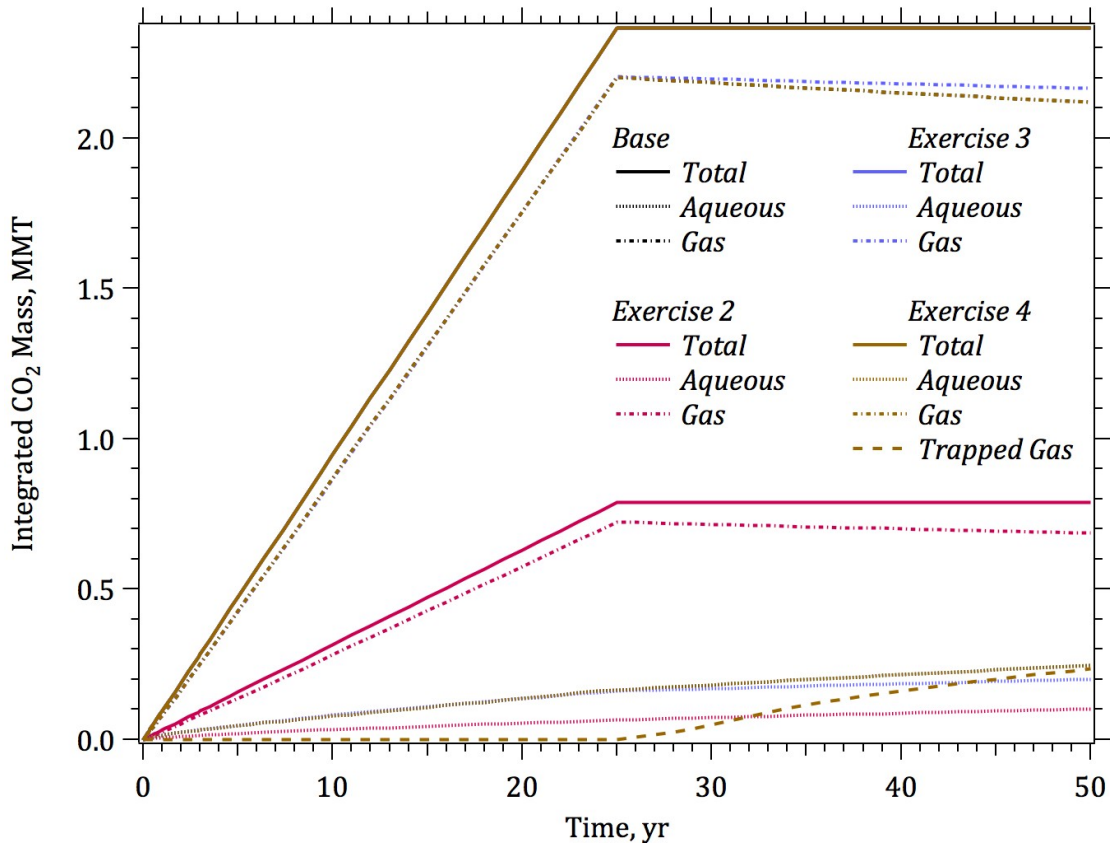


Figure 3. Distribution of CO₂ Mass versus Time for All Exercises

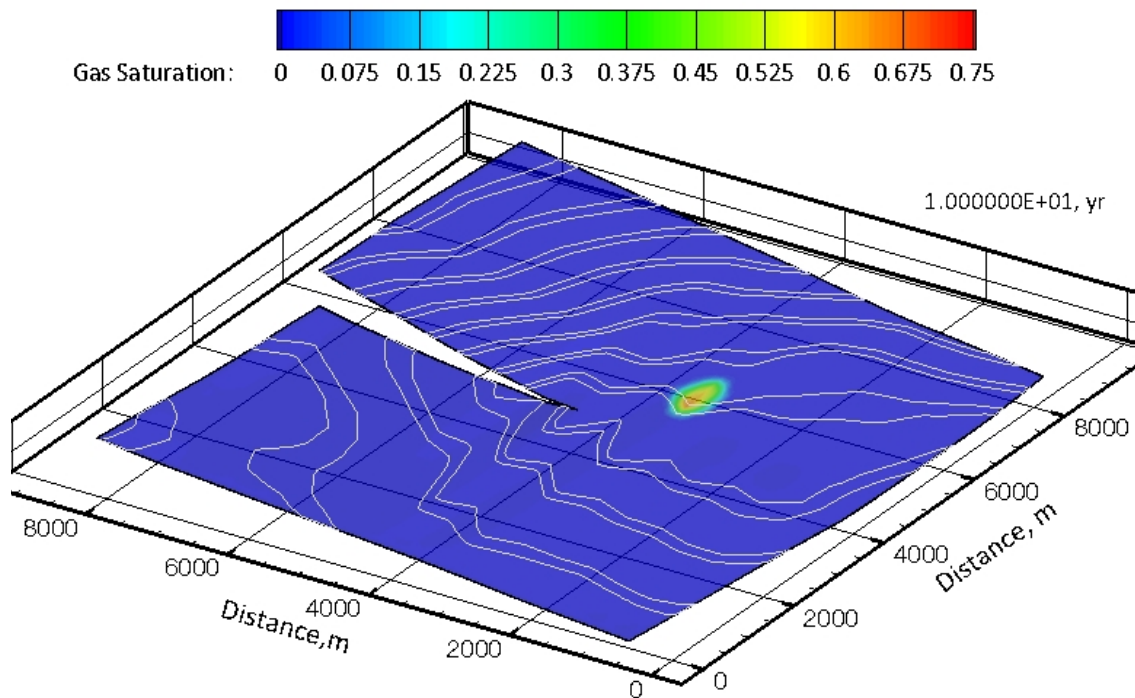


Figure 4a. CO₂ Gas Saturation at 10 years for Exercise 2.

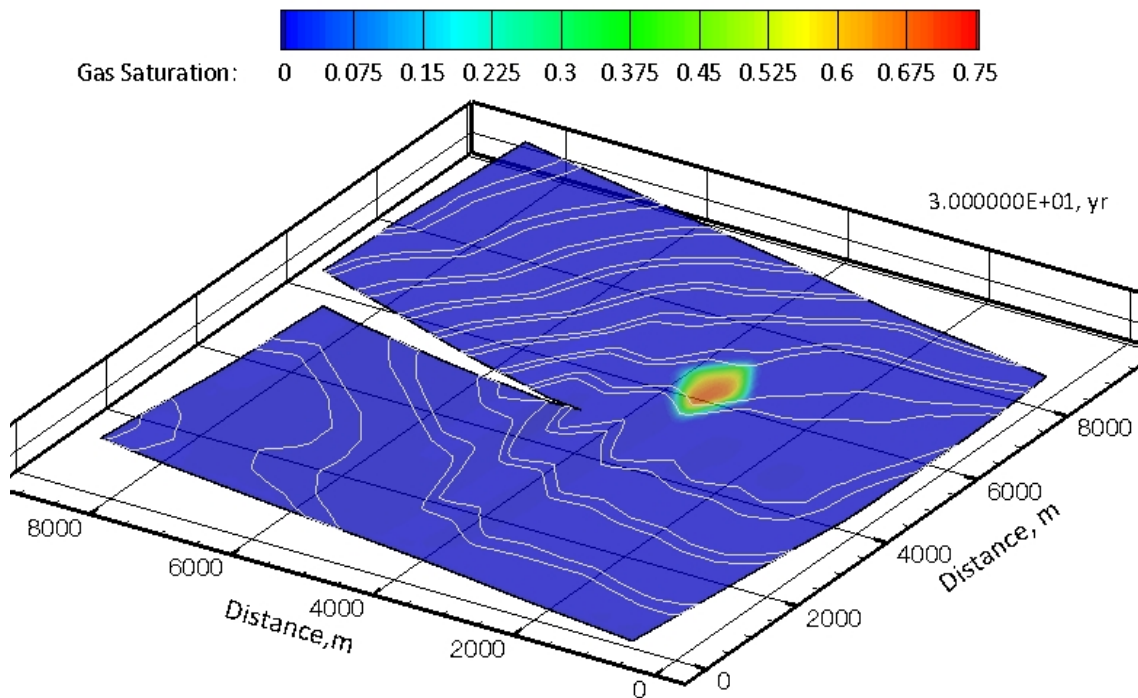
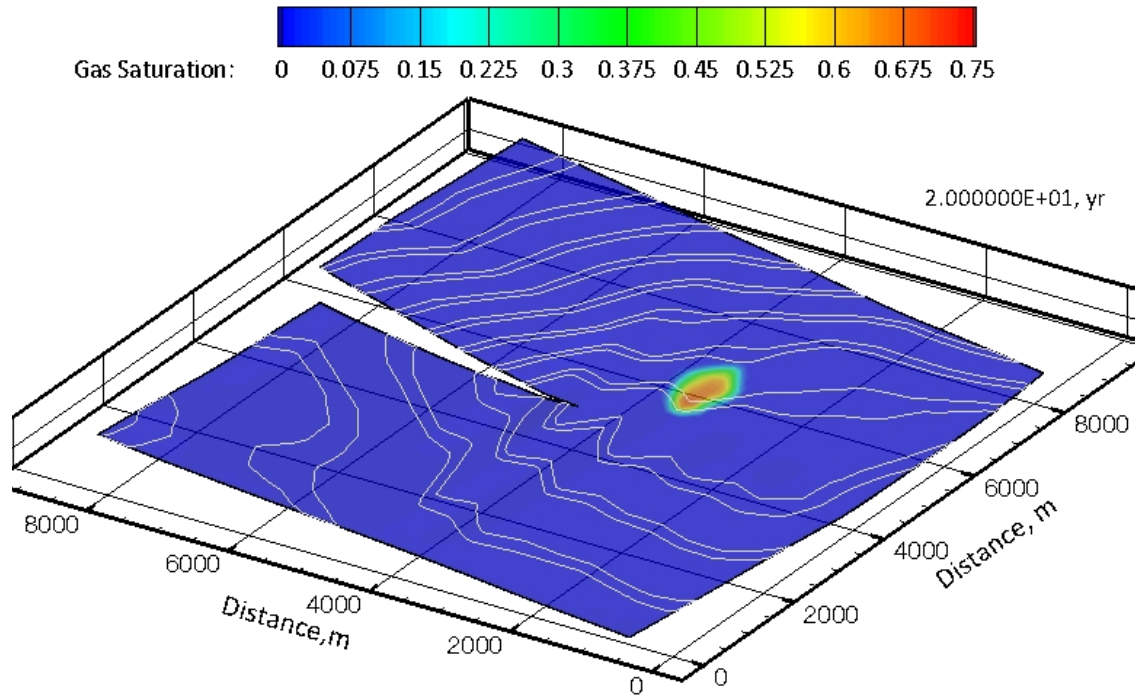


Figure 4b. CO₂ Gas Saturation at 20 and 30 years for Exercise 2.

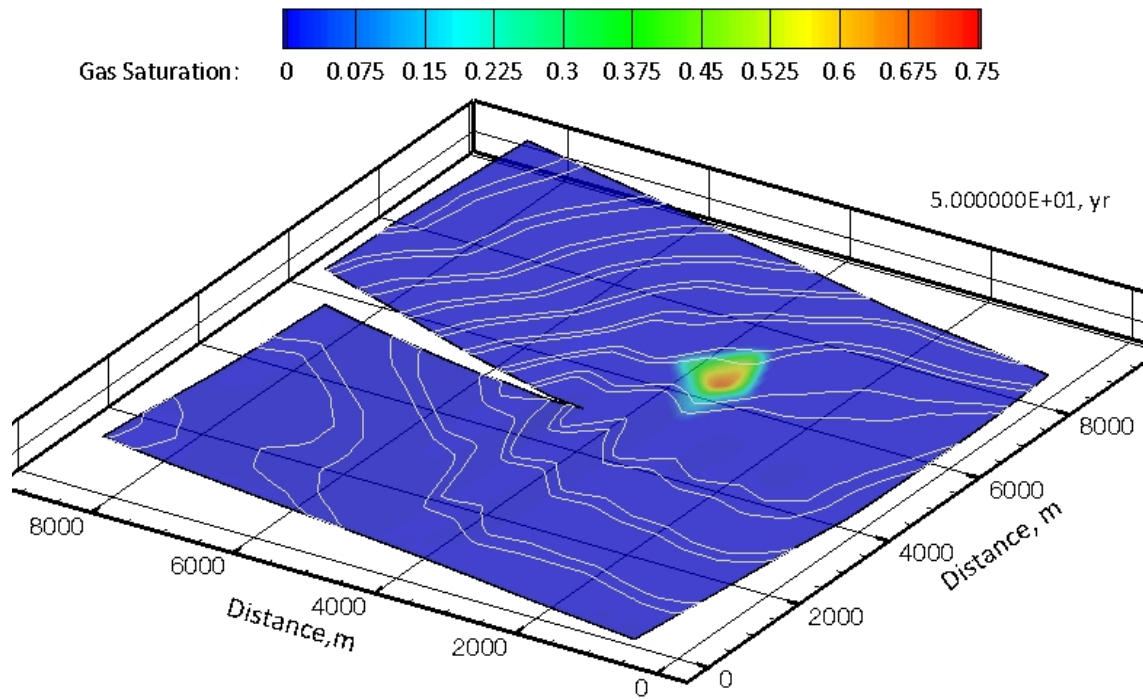
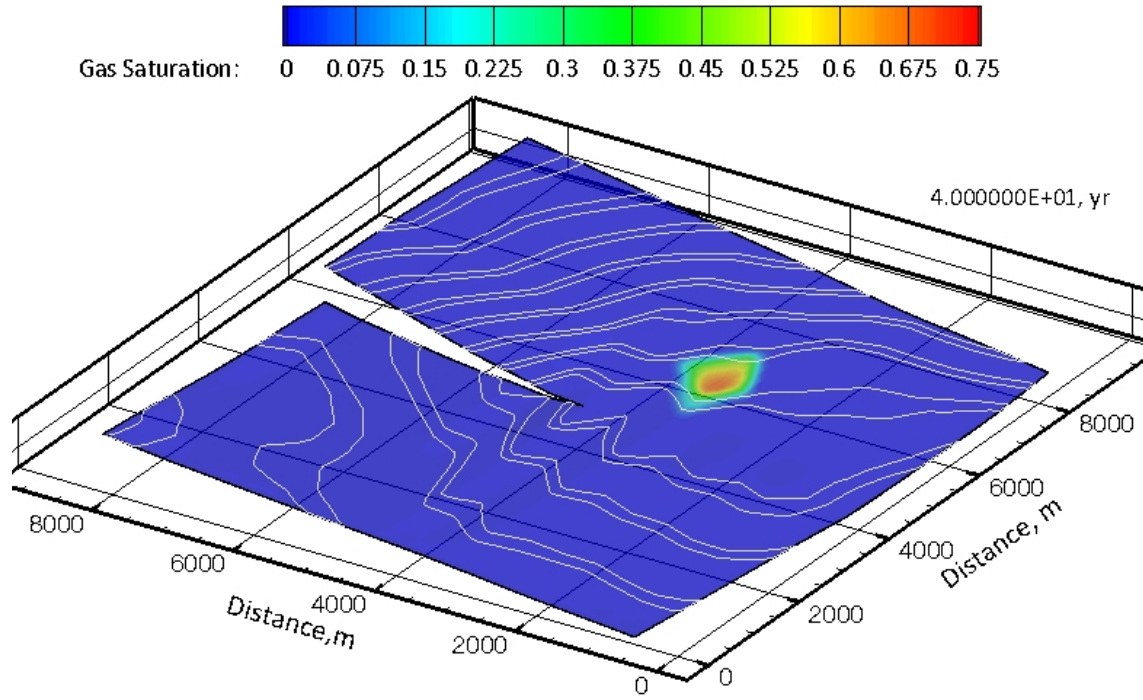


Figure 4c. CO₂ Gas Saturation at 40 and 50 years for Exercise 2.

Exercise 3

The aquifer hydraulic properties can have a significant impact on the amount of CO₂ that a given formation can safely store. In this exercise, the permeability and porosity distributions were changed by specifying properties for a different layer. This short course problem was based on a benchmark problem that originally contained 9 layers. Properties for the base case (Exercise 1) were obtained from layer 9. In this exercise, properties for layer 2 were used to identify differences in storage and migration. This was accomplished by specifying files corresponding to layer 2. Figure 3, shows the impact of changes in permeability and porosity on the distribution of CO₂. The layer 2 properties yield more rapid dissolution of CO₂ in the aqueous phase compared with the layer 9. This enhanced dissolution rate is strictly due to the increased mobility of the CO₂ plume, as shown in the time-series plots of the spatial distribution of the gas saturation show how the plume evolves over time, Figures 5a, 5b, and 5c.

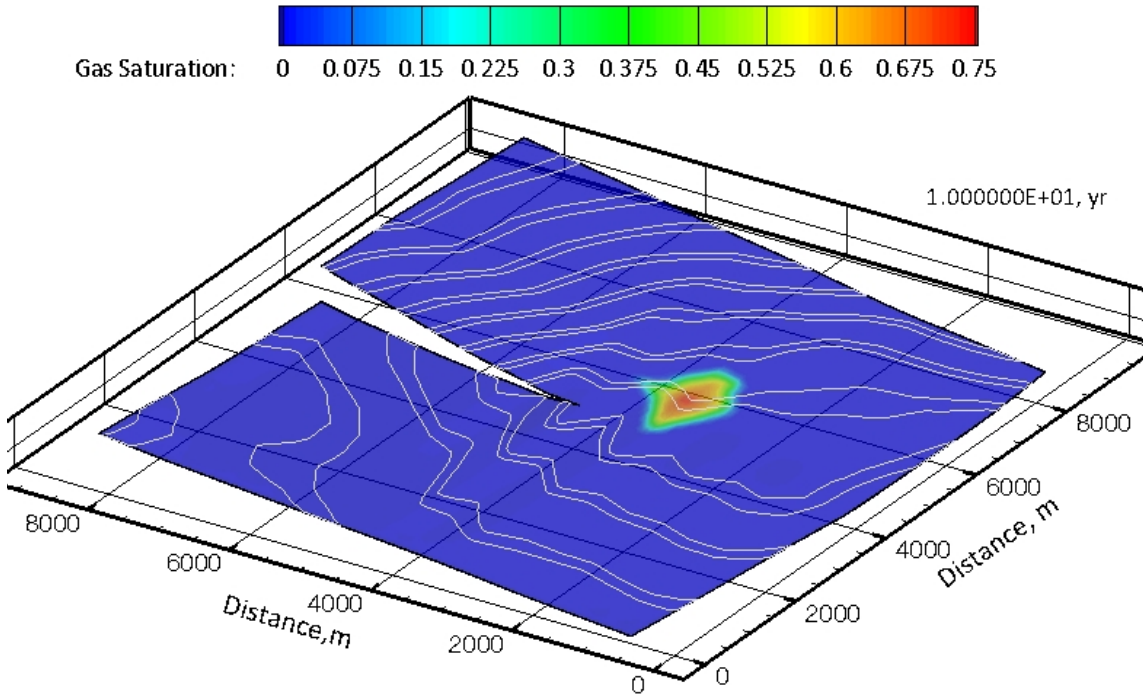


Figure 5a. CO₂ Gas Saturation at 10 years for Exercise 3.

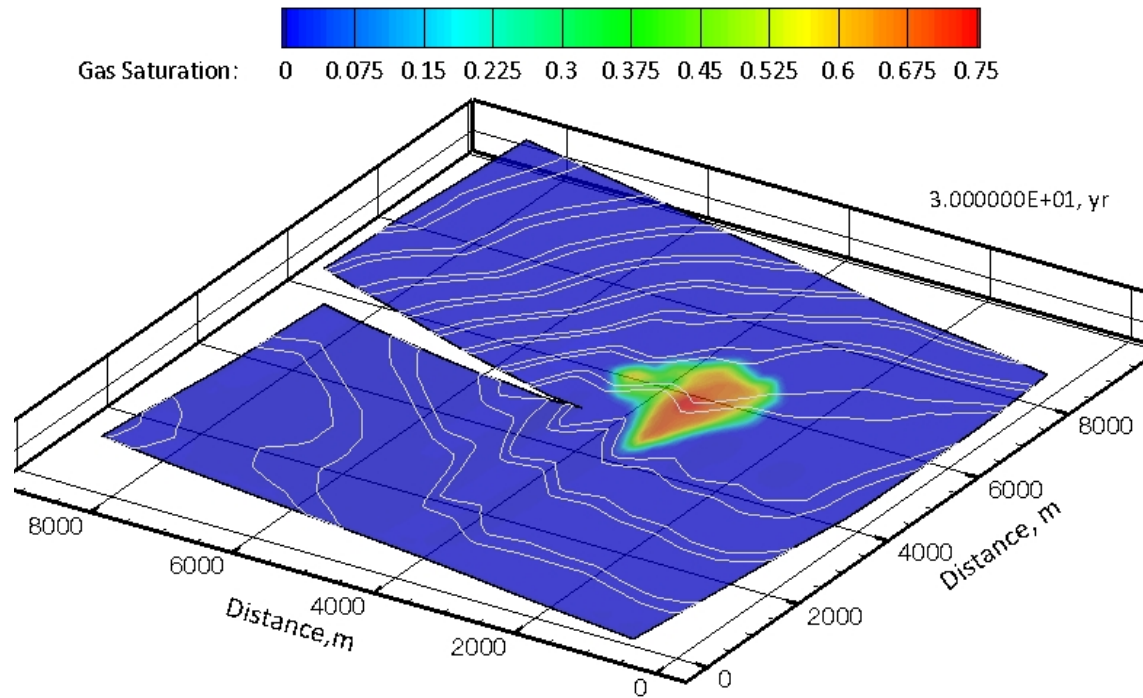
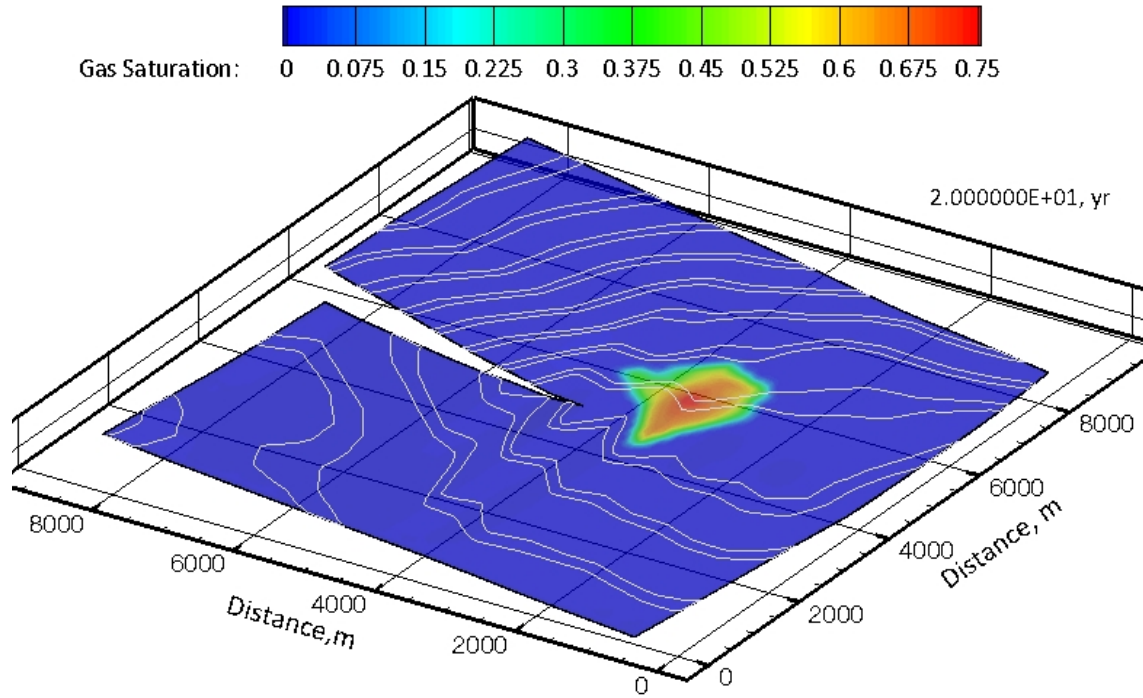


Figure 5b. CO₂ Gas Saturation at 20 and 30 years for Exercise 3.

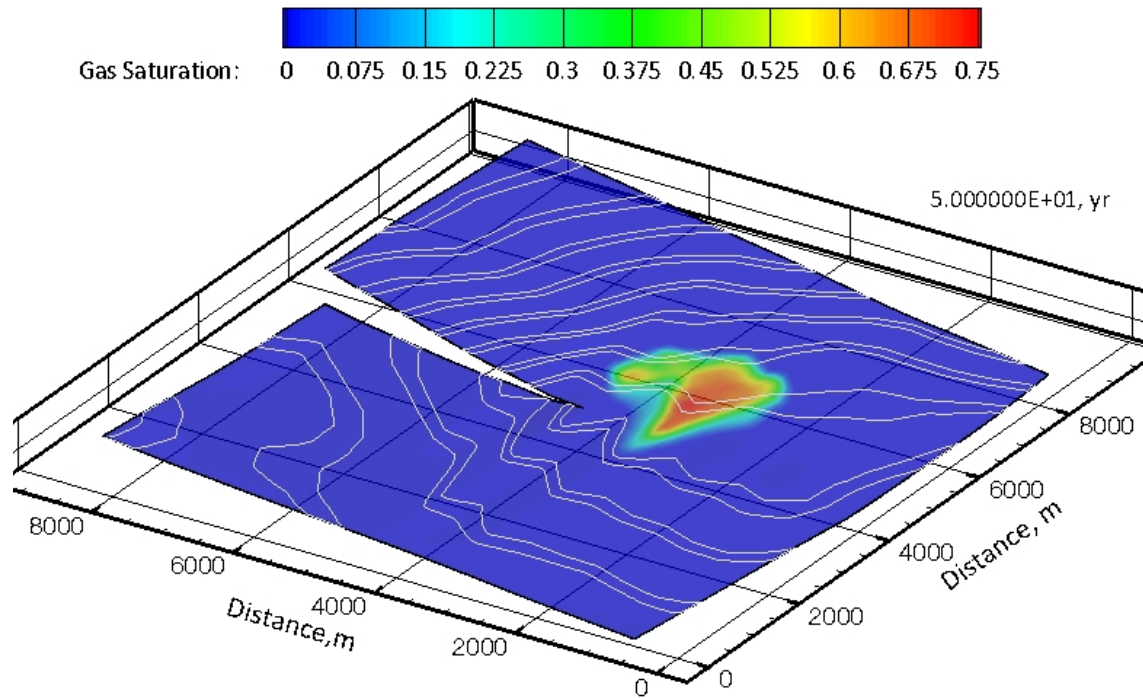
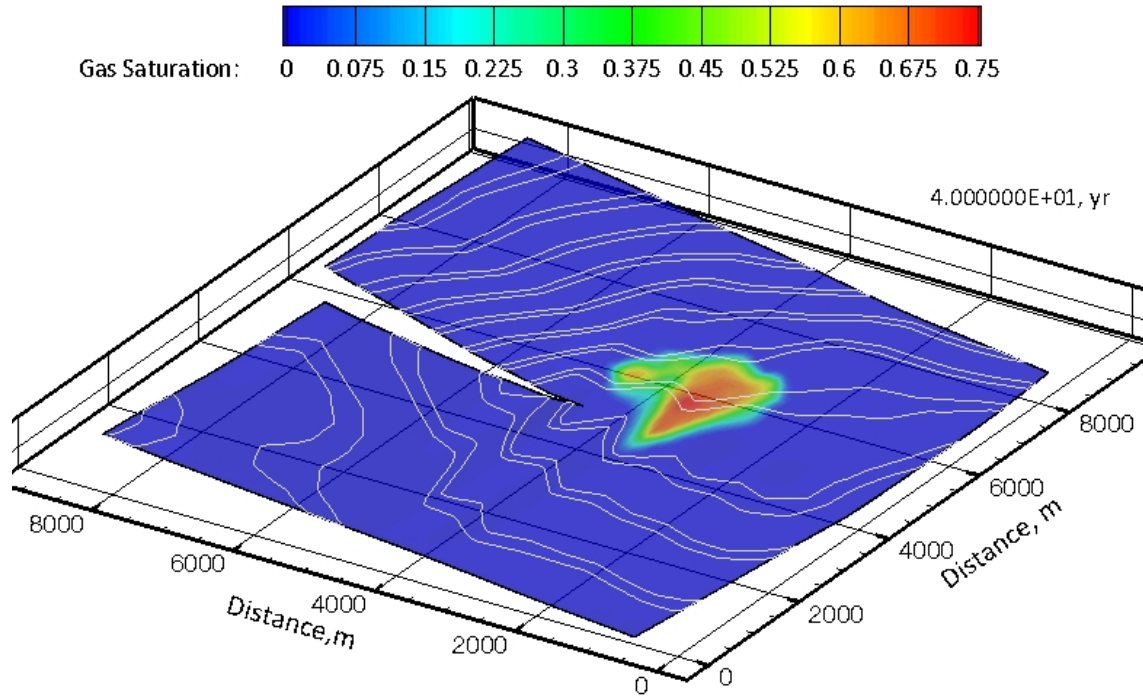


Figure 5c. CO₂ Gas Saturation at 40 and 50 years for Exercise 3.

Exercise 4

Gas entrapment is invoked implicitly through the choice of gas relative permeability functions that include a residual gas saturation parameter, or explicitly by specifying the keyword “Entrapment” as part of the saturation function and then specifying the maximum actual entrapped gas saturation. When entrapment is invoked explicitly the Lands model is used to compute gas entrapment, where the amount of trapped gas is dependent on the point of reversal from drainage to imbibition, the saturation, and the maximum trapped gas saturation. When gas entrapment is invoked explicitly, trapped gas is assumed to be immobile. For this exercise the Saturation Function Card was modified. Figure 3 shows that gas entrapment does not occur until the end of the injection period. The distribution and evolution of trapped gas after the 25-year injection period is shown in the time sequence of plots in Figures 6a and 6b.

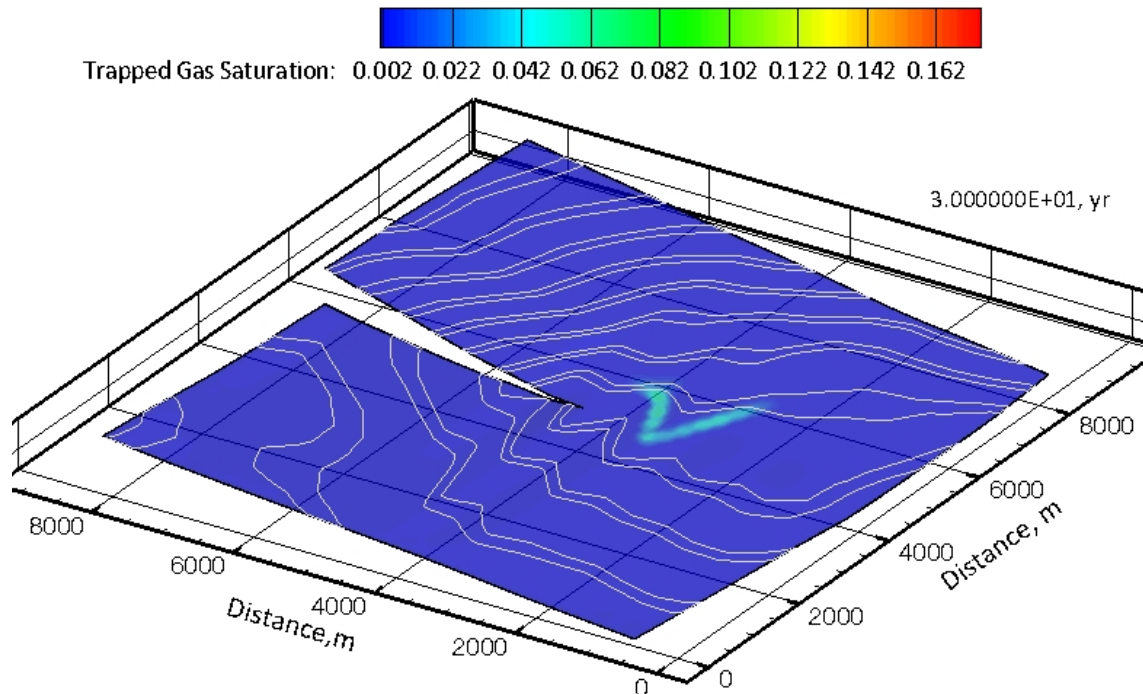


Figure 6a. CO₂ Gas Saturation at 30 years for Exercise 4.

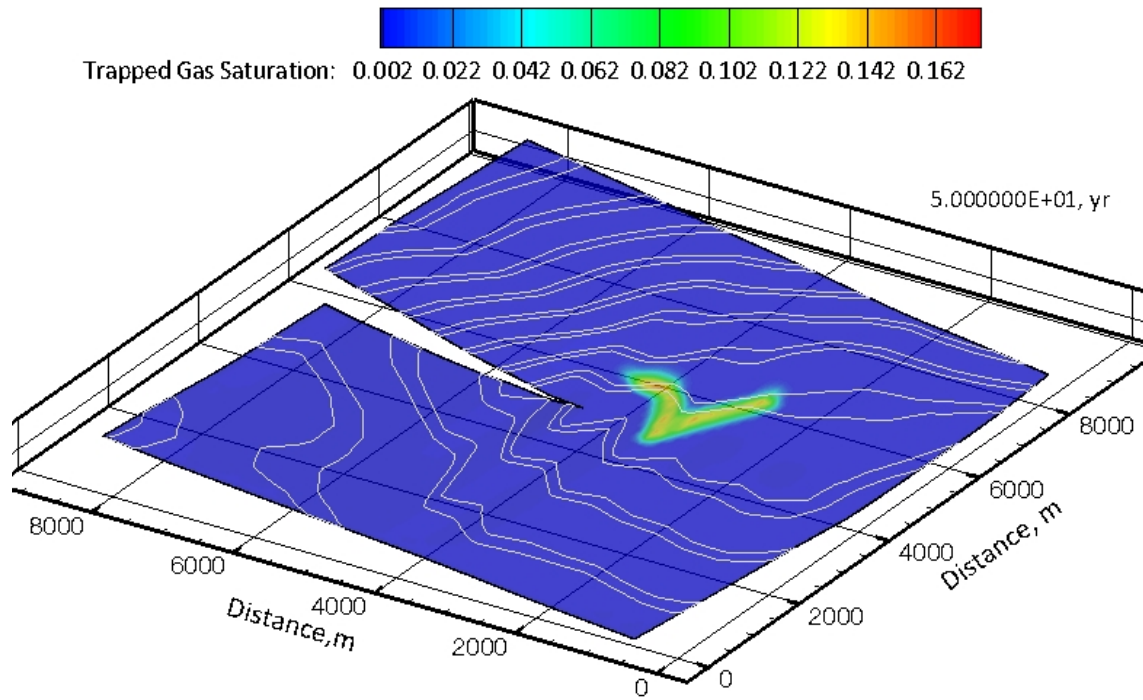
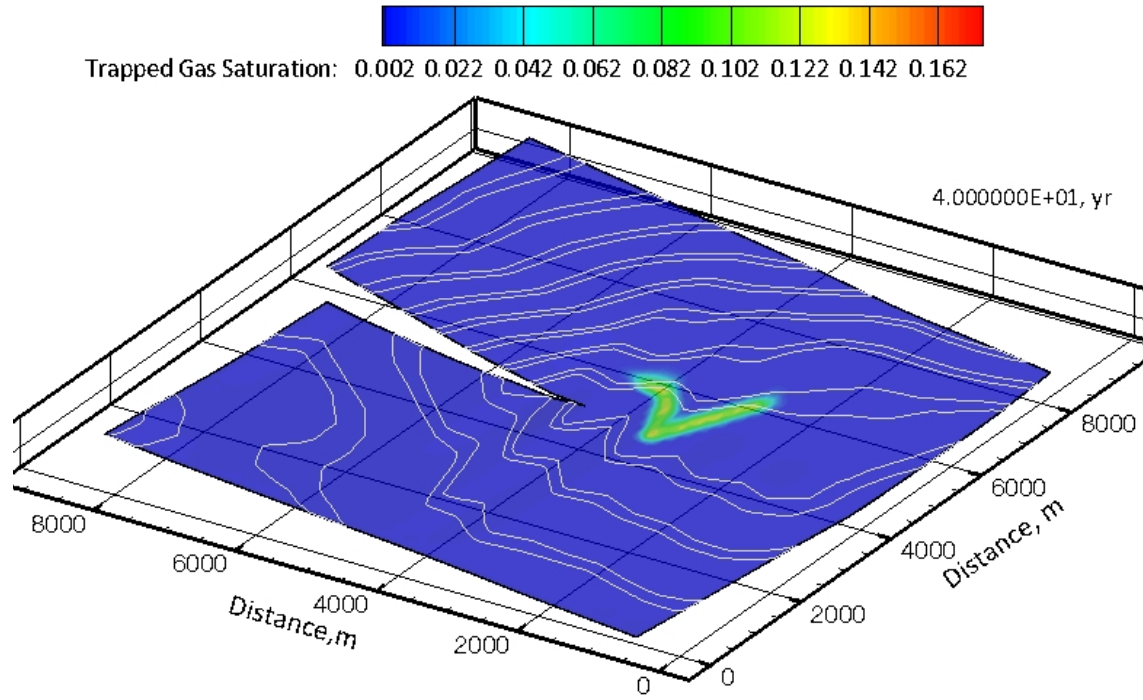


Figure 6b. CO₂ Gas Saturation at 40 and 50 years for Exercise 4.